Future Journal of Pharmaceutical Sciences

RESEARCH

Open Access

Design, synthesis and in-vitro anti-depressant activity evaluation of some 2-styrylbenzimidazole derivatives

Manisha Sahariah[1], Rubina Chowdhury[1], Padmanath Pegu[2], Farak Ali[2], Rajat Subhra Dutta[2] and Supriya Sahu[2*]

Abstract

Background Existing antidepressants possess various adverse effects and so they are not considered as the first line of drug in mild depression. The lack of proper drugs to treat the mild depression on the other hand alleviates severe depressive cases. To overcome this problem, the nucleus of benzimidazole and cinnamic acid having very less toxicity were fused and a small library of 40 compounds was prepared. The library was then screened for ADMET properties and probable toxicity. Those compounds which had not shown any toxicity as well as possessed better *in-silico* absorption, distribution and metabolism were selected for the first phase of the study. Synthesized compounds were characterized by FTIR, ^{1}H-NMR and ^{13}C-NMR and were screened for in-vitro antidepressant activity by DNPH spectrophotometry.

Result The compounds MS-3 and MS-8 had shown good antidepressant activity with IC_{50} values of 367.19 µM/mL and 184.56 µM/mL against MAO-A and MAO-B, respectively.

Conclusion From this study, it can be concluded that the structural requirements for the inhibition of MAO-A and MAO-B were totally different. MAO-A inhibitors required the presence of nitrogen and oxygen containing ring substitutions whereas MAO-B inhibitors required the presence of 4-halogen containing phenyl ring substitutions.

Keywords Antidepressants, Benzimidazole, Monoamine oxidase, Cinnamic acid, Docking

*Correspondence:
Supriya Sahu
supsjrt@gmail.com
Full list of author information is available at the end of the article

Graphical abstract

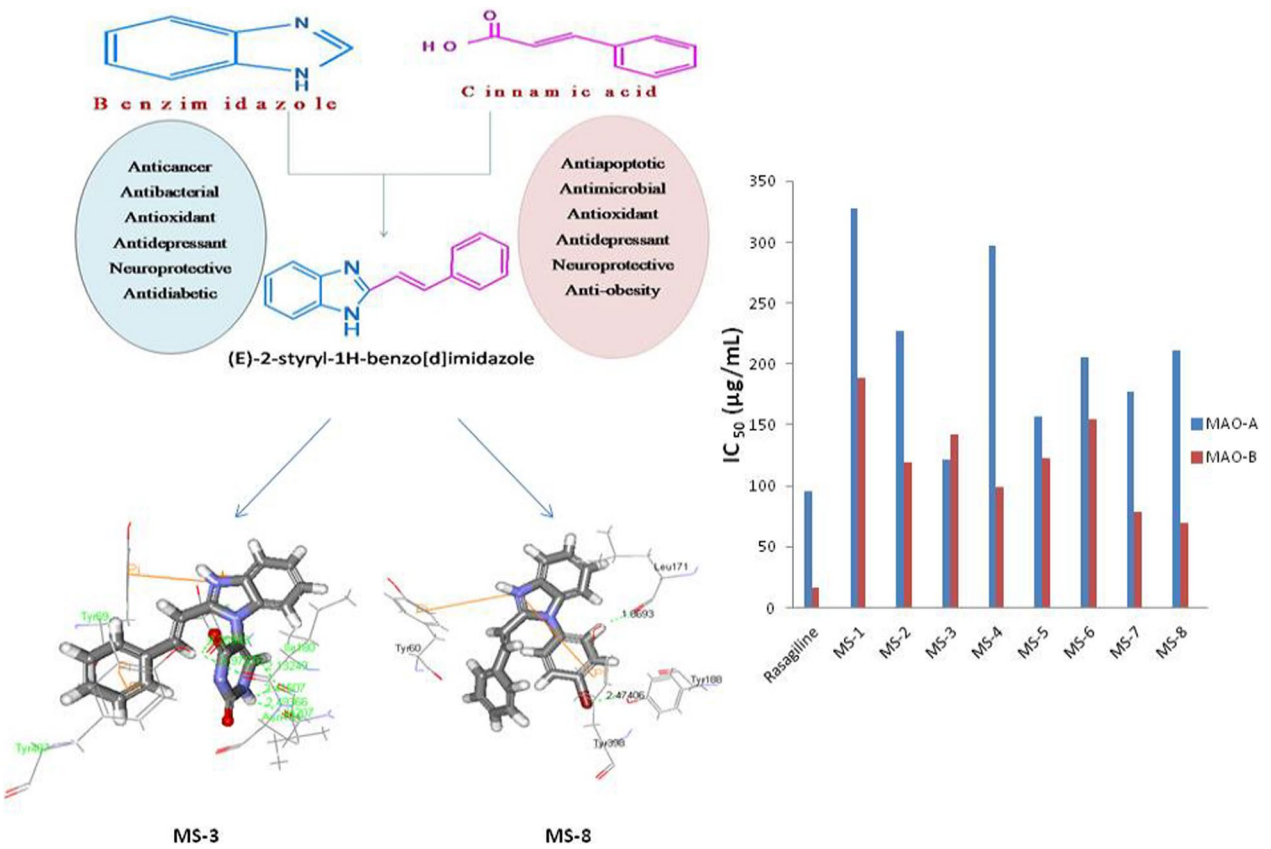

Background

Depression is a life-threatening disease which is characteristically different from normal mood swing and short-lived emotional responses to challenges in everyday life. It causes the suffered person to function poorly in any kind of activity, ultimately leading to suicide, which is the fourth leading cause of death mainly in 15–29 years old. According to the Global Health Data Exchange (GHDx) report, 2019 published by Institute of Health Metrics and Evaluation, depression affects 3.8% of the world's population [1]. Approximately 280 million people in the world have depression, 5.02% of which comes under the age group of 20 plus years and 5.71% of which comes under the age group of 60–89 years [2].

Although there are effective treatments for depression, more than 75% of people who lives in poorer countries receive no treatment. The reason may be low resources, a smaller number of trained healthcare providers and the social stigma associated with a mental disorder. Sometimes it is because of misdiagnosis and many times because of wrongly prescribed anti-depressants. The effective treatments for depression include counselling, cognitive treatment and interpersonal psychotherapy, sometimes along with antidepressant medication such as selective serotonin reuptake inhibitors (SSRIs), 5-HT receptor antagonists (5HT-RAs), monoamine oxidase inhibitors (MAOIs) and tricyclic antidepressants (TCAs). These antidepressants are not considered as the first line of treatment for mild depression mainly because of the adverse effects associated with these classes of antidepressants [2].

As the number of suicidal cases is alarmingly increasing day by day which is evident from the daily newspapers, it is the need of the hour to develop potent antidepressants with minimal adverse effects. To do so, we were in search of some chemical scaffold that has been widely explored as different drug molecules, safe to use and poses minimum side effect. The answer we found is benzimidazole, which is one of the most widely explored chemical moiety having diverse biological activities viz. Antiviral [3–7], antimicrobial [8–11], anticancer [12–16] antidiabetic [17–19] etc. along with some reported anti-depressant

[20, 21] property also. On the other hand, cinnamic acid which is a widely distributed natural aromatic carboxylic acid have gained the attention of researchers due to its low toxicity, structural diversity and pharmacological actions [22] like anti-inflammatory [23], antioxidant [24], antitumor [25], hypoglycaemic [26], antidepressant [27], and cytoprotective actions of neuroinflammation in neurodegenerative diseases [28]. The antidepressant action of cinnamic acid occurs via important neurotransmitter serotonin, which also has similar mechanism of action with many commercial antidepressants [29].

The designed compounds, 2-styrylbenzimidazole derivatives were synthesized by reacting o-phenylenediamine and cinnamic acid. The two amino groups of o-phenylenediamine were fused with the carboxylic group of cinnamic acid leading to the formation of 2-styrylbenzimidazole.

These 2-styryl benzimidazole derivatives were reported to have anti-bacterial, anti-fungal and anti-tubercular activity [30]. Based on these findings and to facilitate the development of less toxic, easily available, more potent antidepressant drugs present study aims at design and synthesis of some novel 2-styrylbenzimidazole derivatives with further investigating their potential as antidepressants using in-vitro methods. The designed compounds were structurally similar to the standard antidepressant drug rasagiline. Therefore, it is believed that the designed compounds will exhibit antidepressant activity by inhibiting the monoamine oxidase enzyme.

Methods

In-silico studies

To test the hypothesis presented in this research paper, we have designed a new series of 2-styrylbenzimidazole derivatives. Direct conjugation of these two chemical scaffolds was not possible. Therefore, we have moved one step back and tried conjugating o-phenylenediamine and cinnamic acid which had resulted in the desired nucleus having the benzimidazole ring as well as the styryl part coming from the cinnamic acid (Fig. 1) exhibiting antidepressant effect. It was evident from literatures that the styryl part which is present in all cinnamic acid similar structures like caffeic acid, ferulic acid, coumaric acid might be responsible for possessing the antidepressant activity [29]. The N^1-hydrogen of the nucleus thus generated was substituted with various aromatic or cyclic halides to get the series of different compounds (Table 1).

Molecular property calculation

Different molecular properties like LogP value (Octanol–water partition coefficient), TPSA (Total Polar Surface Area), molecular weight, nRB (Number of Rotatable Bond), HBD (Hydrogen Bond Donor) and HBA (Hydrogen Bond Acceptor) that are considered under Lipinski's rule of five were determined using the free online software 'molinspiration property calculator.'

ADMET prediction

The series of compounds was then used to calculate the ADMET descriptors (absorption, distribution, metabolism, excretion and toxicity) using Discovery studio 3.1 (Accelrys, San Diego, CA, USA). The descriptors selected for this study are absorption, solubility, AlogP98 and PSA_2D values. The model for plotting the confidence ellipse was developed by Egan and Lauri [31] with descriptors that include AlogP98 and 2D polar surface area (PSA_2D). Aqueous solubility was predicted by using a model developed by Cheng and Merz [32] with $R^2 = 0.84$. All the models used for predicting the ADME, toxicity, AlogP98 and PSA_2D have high R^2 values.

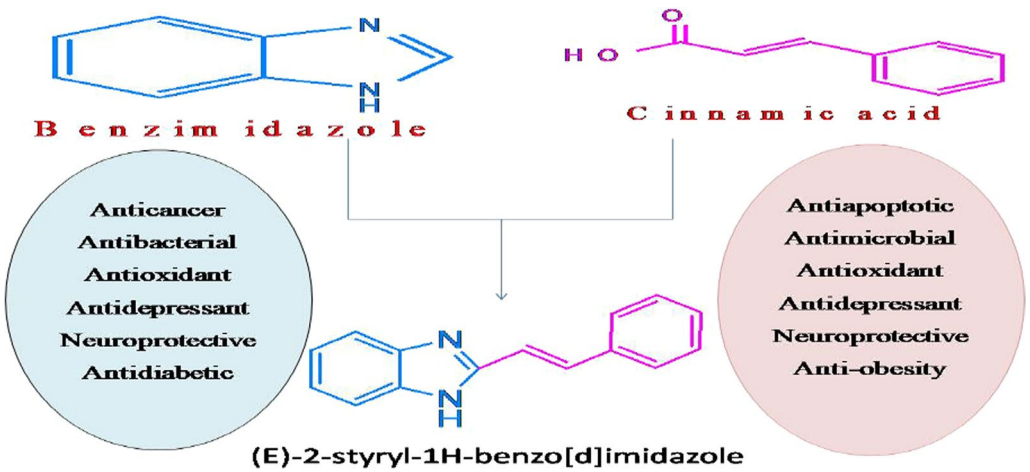

Fig. 1 Benzimidazole cinnamic acid-conjugated nucleus

Table 1 Designed library

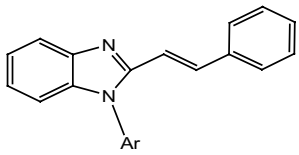

SL No	Compound code	ArX
1	MS1	*4-chlorobenzenamine*
2	MS2	*benzenesulfonyl chloride*
3	MS3	*5-bromouracil*
4	MS4	*3-chloro-4-fluoroaniline*
5	MS5	*N-chlorosuccinimide*
6	MS6	*p-chlorotoluene*
7	MS7	*1,4-dichlorobenzene*
8	MS8	*1,4-dibromobenzene*
9	MS9	*1-(2-chloroethyl)piperidine*
10	MS10	*4-(2-chloroethyl)morpholine*
11	MS11	*(4-chlorophenyl)methanamine*
12	MS12	*4-(chloromethyl)benzenamine*
13	MS13	*1,3-dichlorobenzene*
14	MS14	*4-methylbenzene-1-sulfonyl chloride*
15	MS15	*4-chloropyridine*
16	MS16	*5-chloropyridin-2-amine*
17	MS17	*1-chloro-4-(chloromethyl)benzene*
18	MS18	*1-chloro-3-(chloromethyl)benzene*
19	MS19	*3-(chloromethyl)oxazolidine*
20	MS20	*4-chloro-N,N-dimethylbenzenamine*
21	MS21	*1-chloro-4-methoxybenzene*
22	MS22	*1-chloro-4-(2-chloroethyl)benzene*
23	MS23	*1-(2-chloroethyl)-4-fluorobenzene*
24	MS24	*1-chloro-3-(2-chloroethyl)benzene*
25	MS25	*2,4-dichloro-1-(2-chloroethyl)benzene*
26	MS26	*1-(2-chloroethyl)-2,4-difluorobenzene*
27	MS27	*2-chloropyridine*
28	MS28	*1-chloronaphthalene*
29	MS29	*Chlorobenzene*
30	MS30	*2-chloro-1H-pyrrole*
31	MS31	*2-chlorothiophene*
32	MS32	*1-chloro-2-methylbenzene*
33	MS33	*4-chlorophenol*
34	MS34	*2-chlorophenol*
35	MS35	*1-chloro-4-methoxybenzene*
36	MS36	*1-chloro-4-methylpiperidine*
37	MS37	*1-chloro-4-methylpiperidine*
38	MS38	*1-chloro-4-methylpiperazine*
39	MS39	*1-chloro-4-ethylpiperazine*
40	MS40	*1-chloro-4-nitrobenzene*

AlogP98 and PSA_2D were used for plotting the confidence ellipse. Compounds which were found outside the 95% and 99% ellipse region were poorly absorbed compounds (< 30% absorbed). The series was then taken for prediction of carcinogenicity and skin irritancy by using the TOPKAT module of Discovery studio 3.1 (Accelrys, San Diego, CA, USA).

Docking study

Docking was performed on the crystal structure of MAO-A and MAO-B which were retrieved from Protein Data Bank (PDB). Monoamine oxidase (MAO) inhibitors were a standard class of antidepressants which prevent the removal of neurotransmitters like dopamine, serotonin from brain and make these neurotransmitters available preventing depression. Rasagiline was a standard MAO inhibitor. Since the compounds were designed based on the structure of rasagiline, the docking study was carried out against MAO-A and MAO-B. The structural features of 2-styrylbenzimidazole derivatives revealed in this study would help in understanding their structural activity relationship with MAO as novel antidepressants. The PDB ID of the selected protein was 2Z5X for MAO-A [33] and 1S3E for MAO-B [34]. Prior to docking, each protein was prepared using protein preparation wizard of Discovery studio 3.1 (Accelrys, San Diego, CA, USA). Polar hydrogen atoms were added to the proteins and charges were assigned. All the bound water molecules, other heteroatoms and co-crystallized ligands attached to the protein were removed. Subsequently, the 3D structure of protein was optimized by minimizing the energy using CHARMm force field. 2Z5X consists of chain A only. Binding site of this protein was defined (40.753, 16.779, 14.746) around the binding pocket of the co-crystallized ligand *7-methoxy-1-methyl-9H-pyrido[3,4-b]indole* which was also known as Harmine. 1S3E consists of two identical chains A and B. Chain A was kept for the study and chain B was deleted. Binding site was defined (52.793, 154.645, 25.957) around the binding pocket of the co-crystallized ligand *5-Hydroxy-N-Propargyl-1(R)-Aminoindan* (RHP). Docking was done using the CDOCKER of Discovery studio 3.1 (Accelrys, San Diego, CA, USA) which was priory validated by calculating RMSD between the docked poses and the X-ray pose of the respective co-crystallized ligands.

Chemistry

AR grade chemicals and solvents were used without further purification for doing the synthetic and analytical

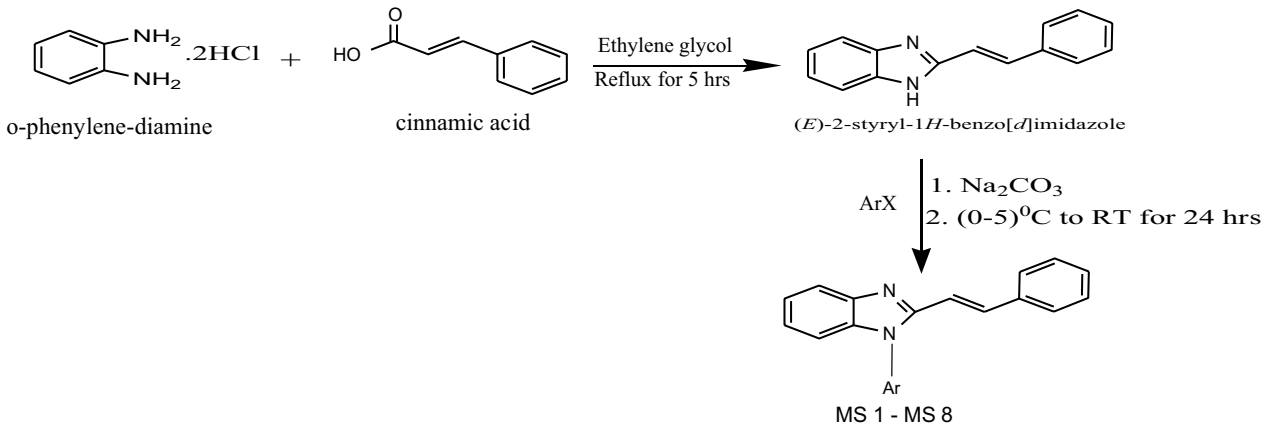

Scheme 1 Synthetic scheme of the compounds MS 1-MS 8

work. Melting point apparatus (BUCHI Melting Point M560) at 10 °C/min temperature gradient was used to determine the melting point of the synthesized compounds. The UV-Spectra (λ_{max}) of the synthesized compounds were recorded on Shimadzu, UV- 1800, UV–VIS spectrophotometer instrument. The FT-IR spectra of the synthesized compounds were recorded on Bruker ALPHA FTIR spectrometer. The ^{1}H-NMR spectra of the synthesized compounds were recorded in DMSO at 300 MHz by Bruker Avance DPX 300 NMR spectrometer and ^{13}C-NMR was also recorded in DMSO at 100 MHz by Bruker Avance DPX 100 NMR spectrometer. The mass spectra of the synthesized compounds were recorded on ZQ-4000 equipped with an Electrospray Ionizer as an ionization method. The eight selected compounds were synthesized by using the scheme 1.

Synthesis of 2-styryl-1H-benzo[d]imidazole

The compound was synthesized by adding cinnamic acid to a mixture of hydrochloric acid and o-phenylenediamine. It was then refluxed in ethylene glycol for 5 h within a temperature range of 70–90 °C. After this, the reaction mixture was cooled to room temperature and poured into water. Resulting solid was filtered, resuspended in water and pH of the solution was adjusted to ≥ 7 using sodium bi -carbonate. The product was filtered, washed, dried and recrystallized with ethanol.

General procedure for synthesis of final compounds

2-styryl-1H-benzo[d]imidazole was dissolved in quantity sufficient THF, basified using sodium carbonate and cooled to (0–5) °C in ice-bath. The respective aryl/cyclic amine was added slowly maintaining the temperature range of (0–5) °C for additional 15 min. Thereafter the media was warmed upto room temperature and stirred for 24 h followed by solvent evaporation. Cold water was added to the resulting mass, filtered and air-dried to obtain the crude product.

In-vitro anti-depressant activity screening

Isolation and preparation of MAO sample

MAO was isolated using brain tissues of chicken. The dissected pieces of the brain tissues were washed with 0.3 M sucrose solution and frozen at − 80 °C for further analysis. The brain tissue (2.5 g) was homogenized in 1:40 (w/v) ratio with 0.3 M ice-cold sucrose solution and centrifuged at 1824 g for 10 min. The supernatant was collected and further centrifuged at 12,768 g for 35 min to obtain crude MAO protein precipitations. This precipitate was resuspended in 250 ml of 0.3 M sucrose solution and mixed with 20 ml of 1.2 M sucrose solution. The precipitate was again centrifuged with 1.2 M sucrose solution at 12,687 g for 40 min followed by a single wash with potassium phosphate buffer (pH 7.60, 100 mM). The pure brain MAO protein precipitate was suspended in 10 ml of potassium phosphate buffer; and stored in aliquots of 1 ml at − 80 °C for subsequent analysis [22, 23].

Determination of protein concentration

The protein concentration of MAO precipitate was calculated using Hartree Lowry method [24–26]. Serial dilutions of concentrations 0.03 to 0.15 mg/ml were prepared from the stock solution of 0.3 mg/ml bovine serum albumin (BSA) in potassium phosphate buffer. 1.0 ml of each dilution of standard, protein-containing test and buffer for reference were mixed with 0.90 ml of reagent A (2 g sodium potassium tartrate, 100 g sodium carbonate, 500 ml 1N NaOH, and water to one liter) in separate test tubes. The tubes were incubated for 10 min in water bath at 50 °C, then cooled to room temperature. 0.1 ml

of reagent B (2 g sodium potassium tartrate, 1 g copper sulfate, 90 ml H_2O and 10 ml 1N NaOH) was added to each test tube, mixed and incubated for 10 min at room temperature. 3 ml of reagent C (1 vol of Folin–Ciocalteau reagent diluted with 15 vols of water) was added rapidly to each test tube, mixed and again incubated for 10 min in water bath at 50 °C and cooled to room temperature. The final assay volume was 5 ml. Absorbance was measured at 650 nm.

DNPH spectrophotometry

Potassium phosphate buffer (pH 7.60, 25 mM) and 200 µL of MAO protein homogenates were mixed and incubated for 20 min at 37 °C. Then 200 ml of 0.016 M benzylamine in buffer (for detecting MAO-B) and 150 ml of 0.02 M 5-HT (for detecting MAO-A) were added to the above mixture and incubated for 60 min. After this 400 ml of 2 M DNPH in 1 M HCl was added. After incubation for 40 min at room temperature, 2 ml of 1.25 M NaOH containing 5 g/l of Triton X-100 was added and the reaction mixture was kept for an additional 30 min at room temperature. Finally, absorption was measured at 465 nm for MAO-B and 425 nm for MAO-A.

Results

In-silico studies

The designed library was screened through lipinsky rule of five by calculating molecular properties and filtered through ADMET prediction filter. Only those compounds which have passed through both these filters were selected for docking, synthesis and in-vitro antidepressant activity evaluation.

Molecular property calculation

Out of the forty compounds of the library, 23 had shown one violation of lipinsky rule whereas remaining 17 compounds had not shown any violations and taken for further screening (Table 2).

ADMET prediction

All the compounds of the designed library fall inside 95% and 99% ellipse region (Fig. 2). From the results of TOPKAT toxicity prediction, it was observed that no compounds had shown carcinogenicity but all except eight had shown mild skin irritancy (Table 3). Thus, only eight compounds of the series had passed all the filters and so they were considered for further studies.

Docking study

Based on the molecular properties and ADMET studies of all the designed ligands, eight compounds were selected for molecular docking studies. Docking is considered to be successful if the RMSD value between the X-ray pose and the docked pose is less than 2 Å [35]. The RMSD value of Harmine and RHP against 2Z5X and 1S3E is tabulated in Tables 4 and 5. The docking results were analyzed based on the binding energy (Table 6) and the docked poses against MAO-A (2Z5X) (Fig. 3) and MAO-B (1S3E) (Fig. 4). The binding energies of the ligands were within the range of − 114.89 to − 53.32 kcal/mol. The ligands showed very high negative binding energies as compared to the standard Harmine/RHP.

Chemistry

Intermediate compound: FT-IR (cm^{-1})

1449.16 (C=C stretch, aromatic), 1578.95 (C–C stretch, aromatic), 1305.12 (C-N stretch, aromatic), 2967.44 (N–H stretch, secondary), 1630.86 (C=C stretch, aliphatic), 2879.02 (C-H stretch, aliphatic), 681.16 (C-H bend, aromatic).

((E)-4-(2-styryl-1H-benzo[d]imidazol-1-yl)benzenamine) (MS-1)

Solubility: Ethanol, DMSO; **R_f value**: 0.38; **M.P:** 115–117 °C; **UV λ_{max}** (DMSO): 253; **FTIR** (cm^{-1}): 1446.67 (C=C stretch, aromatic), 1625.38 (C–C stretch, aromatic), 1281.60 (C-N stretch, aromatic), 2968.09 (C-H stretch, aromatic), 3418.46 (N–H stretch, primary), 1668.09 (C=C stretch, aliphatic), 2878.54 (C-H stretch, aliphatic), 764.59 (C-H bend, aromatic).**^{1}H NMR** (300 MHz, DMSO): δ, ppm: 5.23 (s, 2H, C-NH), 6.56, (d, J=6 Hz, 2H, arom. H), 7.01 (d, J=6 Hz, 2H, Ethylene), 7.37 (t, J=3 Hz, 3H, arom. H), 7.44 (d, J=6 Hz, 4H, Aniline), 7.68 (t, J=3 Hz 2H, Benzimidazole), 7.61 (d, J=6 Hz, 2H, Benzimidazole). **^{13}C NMR** (100 MHz, DMSO-*d6*) δ ppm: 142.73, 135.52, 123.92, 112.46, 133.82, 128.96, 131.30, 117.61, 124.75, 152.07. **Mass:** 312.15 $(M+H)^+$ (Tables 7 and 8).

((E)-1-(phenylsulfonyl)-2-styryl-1H-benzo[d]imidazole) (MS-2)

Solubility: Ethanol, DMSO; **R_f value**: 0.45; **M.P**: 215–218 °C; **UV λ_{max}** (Ethanol): 274.902; **FTIR** (cm^{-1}): 1447.59 (C=C stretch, aromatic), 1626.22 (C–C stretch, aromatic), 1282.65 (C-N stretch, aromatic), 2967.50 (C-H stretch, aromatic), 1671.62 (C=C stretch, aliphatic), 2878.27 (C-H stretch, aliphatic), 764.19 (C-H bend, aromatic) 1416.27 (S=O stretch, sulfoxide). **^{1}H NMR** (300 MHz, DMSO): δ, ppm: 6.54, (d, *J*=9 Hz, 2H, arom. H), 7.64 (*d*, *J*=6 Hz, 2H, Ethylene), 7.33 (*t*, *J*=3 Hz, 3H, arom. H), 7.44 (*d*, *J*=6 Hz, 2H, Sulfonyl benzene), 7.55 (*t*, *J*=3 Hz, 3H, Sulfonyl benzene), 7.77 (*t*, *J*=3 Hz 2H, Benzimidazole), 7.68 (*d*, *J*=6 Hz, 2H, Benzimidazole). **^{13}C NMR** (100 MHz, DMSO-*d6*) δ ppm: 142.02, 137.19, 135.70, 116.39. **Mass:** 361.09 $(M+H)^+$.

Table 2 Molecular properties of designed ligands

Compound code	miLogP	TPSA	nAtoms	MW	nHBA	nHBD	nNiolations	nRB
MS1	4.33	43.85	24	311.39	3	2	0	3
MS2	4.89	51.97	26	360.44	4	0	0	4
MS3	2.99	83.55	25	330.35	6	2	0	3
MS4	4.85	43.85	25	329.38	3	2	0	3
MS5	3.03	55.21	24	317.35	5	0	0	3
MS6	4.92	17.83	24	310.4	2	0	0	3
MS7	4.65	17.83	24	330.82	2	0	0	3
MS8	4.39	17.83	24	375.27	2	0	0	3
MS9	5.7	21.06	25	331.46	3	0	1	5
MS10	3.86	30.30	25	333.44	4	0	0	5
MS11	4.44	43.85	25	325.42	3	2	0	4
MS12	5.93	43.85	25	325.42	3	2	1	4
MS13	6.12	17.83	24	330.82	2	0	1	3
MS14	5.34	51.97	27	374.46	4	0	1	4
MS15	6.06	30.72	23	297.36	3	0	1	3
MS16	4.22	56.74	24	312.38	4	2	0	3
MS17	6.25	17.83	25	344.85	2	0	1	4
MS18	6.23	17.83	25	344.85	2	0	1	4
MS19	3.83	30.30	23	305.38	4	0	0	4
MS20	5.36	21.06	26	339.44	3	0	1	4
MS21	5.31	27.06	25	326.40	3	0	1	4
MS22	6.04	17.83	26	358.87	2	0	1	5
MS23	5.95	17.83	26	342.42	2	0	1	5
MS24	6.44	17.83	26	358.87	2	0	1	5
MS25	7.07	17.83	27	393.32	2	0	1	5
MS26	6.04	17.83	27	360.41	2	0	1	5
MS27	4.78	30.72	23	297.36	3	0	0	3
MS28	6.63	17.83	27	346.43	2	0	1	3
MS29	5.25	17.83	23	296.37	2	0	1	3
MS30	4.72	33.62	22	285.35	3	1	0	3
MS31	5.46	17.83	22	302.40	2	0	1	3
MS32	5.87	17.83	24	310.40	2	0	1	3
MS33	4.78	38.05	24	312.37	3	1	0	3
MS34	5.20	38.05	24	312.37	3	1	1	3
MS35	5.31	27.06	25	326.40	3	0	1	4
MS36	4.89	21.06	23	303.41	3	0	0	3
MS37	5.13	21.06	24	317.44	3	0	1	3
MS38	3.88	24.30	24	318.42	4	0	0	3
MS39	6.25	17.83	25	344.85	2	0	1	4
MS40	5.21	63.65	26	341.37	5	0	1	4

((E)-5-(2-styryl-1H-benzo[d]imidazol-1-yl) pyrimidine-2,4(1H,3H)-dione) (MS-3)

Solubility: Ethanol, DMSO; **R_f value**: 0.26; **M.P:** 189 °C; **UV λ_{max}** (Ethanol): 260.60; **FTIR** (cm^{-1}): 1425.64 (C=C stretch, aromatic), 1526.05 (C–C stretch, aromatic), 1278.92 (C-N stretch, aromatic), 3054.26 (C–H stretch, aromatic), 1644.69 (C=C stretch, aliphatic), 2882.33 (C–H stretch, aliphatic), 739.88 (C-H bend, aromatic), 3389.24 (N–H stretch, primary), 1745.86 (C=O stretch, ketone). **^{1}H NMR** (300 MHz, DMSO): δ, ppm: 12.63 (s, 1H pyrimidine NH), 7.19 (s, 1H pyrimidine NH), 7.25 (s, 1H pyrimidinyl H), 7.20 (*d*, *J* = 3 Hz, 2H, arom. H), 7.37 (*d*, *J* = 3 Hz, 2H, Ethylene), 7.46 (*t*, *J* = 3 Hz, 3H, arom. H), 7.67 (*t*, *J* = 6 Hz 2H, Benzimidazole), 7.60

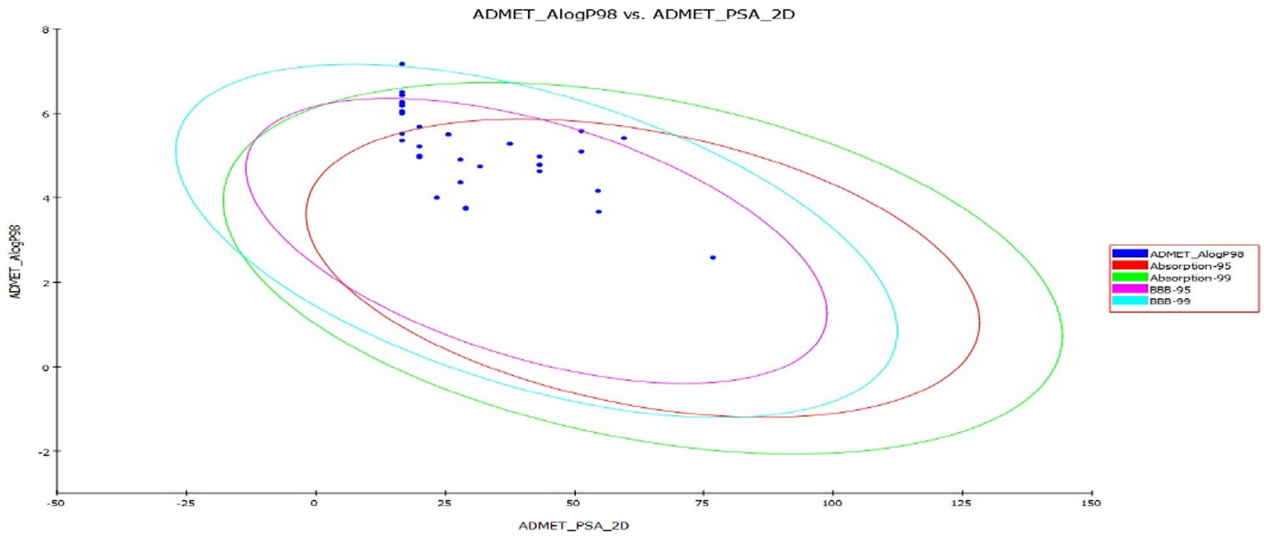

Fig. 2 Confidence ellipse plot

(d, J = 6 Hz, 2H, Benzimidazole). **^{13}C NMR** (100 MHz, DMSO-*d6*) δ ppm: 140.85, 135.75, 129.07, 150.28, 158.80, 113.27, 115.29, 119.48. **Mass:** 331.11 $(M+H)^+$.

((E)-4-fluoro-3-(2-styryl-1H-benzo[d]imidazol-1-yl) benzenamine) (MS-4)

Solubility: Ethanol, DMSO; **R_f value**: 0.79; **M.P:** 180–182 °C; **UV λ_{max}** (Ethanol): 219.40/ 262.20; **FTIR** (cm^{-1}): 1503.72 (C=C stretch, aromatic), 1577.32 (C–C stretch, aromatic), 1272.79 (C-N stretch, aromatic), 3023.42 (C-H stretch, aromatic), 1638.71 (C=C stretch, aliphatic), 2973.94 (C-H stretch, aliphatic), 743.72 (C–H bend, aromatic), 1223.22 (C–F stretch, halogen), 3056.78 (N–H stretch, primary). **^{1}H NMR** (300 MHz, DMSO): δ, ppm: 3.32 (s, 2H, NH_2, floroaniline), 7.15 (s, 1H, floroaniline), 7.20 (*d*, *J* = 3 Hz, 1H, floroaniline), 7.18 (*d*, *J* = 3 Hz, 1H, floroaniline), 7.23 (*d*, *J* = 12 Hz, 2H, arom. H), 7.49 (*d*, *J* = 6 Hz, 2H, Ethylene), 7.45 (*t*, *J* = 3 Hz, 3H, arom. H), 7.67 (*t*, *J* = 6 Hz 2H, Benzimidazole), 7.60 (*d*, *J* = 3 Hz, 2H, Benzimidazole). **^{13}C NMR** (100 MHz, DMSO-*d6*) δ ppm: 142.38, 135.67, 128.07, 133.59, 146.38, 123.97, 150.46, 115.93, 146.39. **Mass:** 330.14 $(M+H)^+$.

((E)-1-(2-styryl-1H-benzo[d]imidazol-1-yl) pyrrolidine-2,5-dione) (MS-5)

Solubility: Ethanol, DMSO; **R_f value**: 0.76; **M.P:** 130–134 °C; **UV λ_{max}** (Ethanol): 262.80; **FTIR** (cm^{-1}): 1420.47 (C = C stretch, aromatic), 1522.82 (C–C stretch, aromatic), 1275.16 (C-N stretch, aromatic), 3026.31 (C-H stretch, aromatic), 1639.45 (C = C stretch, aliphatic), 2923.04 (C-H stretch, aliphatic), 741.21 (C-H bend, aromatic), 1701.75 (C = O stretch, ketone). **^{1}H NMR** (300 MHz, DMSO): δ, ppm: 2.42 (t, J = 3 Hz, 4H, pyrrolidone CH), 7.24 (d, J = 3 Hz, 2H, arom. H), 7.40 (d, J = 6 Hz, 2H, Ethylene), 7.46 (t, J = 6 Hz, 3H, arom. H), 7.58 (t, J = 3 Hz 2H, Benzimidazole), 7.70 (d, J = 3 Hz, 2H, Benzimidazole). **^{13}C NMR** (100 MHz, DMSO-*d6*) δ ppm: 139.90, 133.56, 129.44, 132.60, 132.88, 171.35, 128.96. **Mass:** 318.12 $(M+H)^+$.

((E)-2-styryl-1-p-tolyl-1H-benzo[d]imidazole) (MS-6)

Solubility: Ethanol, Acetone, DMSO, 1,4-dioxane; **R_f value:** 0.81; **M.P:** 187–190 °C; **UV λ_{max}** (Ethanol): 262.40; **FTIR** (cm^{-1}): 1419.06 (C = C stretch, aromatic), 1522.88 (C–C stretch, aromatic), 1274.73 (C-N stretch, aromatic), 3058.58 (C-H stretch, aromatic), 1642.43 (C = C stretch, aliphatic), 2979.18 (C-H stretch, aliphatic), 746.76 (C-H bend, aromatic). **^{1}H NMR** (300 MHz, DMSO): δ, ppm: 2.52 (s, 3H, CH_3-toluene), 7.23 (d, J = 3 Hz, 4H, Toluene), 7.18 (d, J = 3 Hz, 2H, arom. H), 7.37 (d, J = 3 Hz, 2H, Ethylene), 7.45 (t, J = 3 Hz, 3H, arom. H), 7.67 (t, J = 3 Hz 2H, Benzimidazole), 7.55 (d, J = 3 Hz, 2H, Benzimidazole). **^{13}C NMR** (100 MHz, DMSO-*d6*) δ ppm: 137.51, 136.56, 128.96, 133.31, 137.51, 123.92, 129.44, 135.89, 112.46. **Mass:** 311.15 $(M+H)^+$.

((E)-1-(4-chlorophenyl)-2-styryl-1H-benzo[d]imidazole) (MS-7)

Solubility: Ethanol, DMSO; **R_f value:** 0.26; **M.P:**175–177 °C; **UV λ_{max}** (Ethanol): 208.60; **FTIR** (cm^{-1}): 1423.61 (C=C stretch, aromatic), 1522.54 (C–C stretch, aromatic), 1277.75 (C-N stretch, aromatic), 3051.80 (C-H stretch, aromatic), 1643.65 (C=C stretch, aliphatic), 2981.48 (C-H stretch, aliphatic), 736.25 (C-H bend, aromatic), 687.74 (C–Cl stretch, halogen). **^{1}H NMR** (300 MHz, DMSO): δ, ppm: 7.18 (d, J = 3 Hz, 4H, chlorobenzene), 7.52 (d,

Table 3 Toxicity, solubility, drug likeliness accounted by TOPKAT in Discovery Studio 3.1

Compound code	ADMET solubility level	ADMET absorption level	ADMET AlogP98	ADMET PSA 2D	Carcinogenicity	Skin irritancy
MS 1	2	0	4.774	43.149	–	–
MS 2	1	0	5.095	51.21	–	–
MS 3	2	0	2.578	76.831	–	–
MS 4	1	0	4.979	43.149	–	–
MS 5	1	0	3.664	54.563	–	–
MS 6	1	1	6.007	16.609	–	–
MS 7	1	1	6.185	16.609	–	–
MS 8	1	1	6.269	16.609	–	–
MS9	1	0	6.269	16.609	–	Mild
MS10	1	1	5	19.961	–	Mild
MS11	2	0	6.192	16.609	–	Mild
MS12	1	1	3.735	28.891	–	Mild
MS13	1	0	5.683	19.961	–	Mild
MS14	1	1	5.504	25.539	–	Mild
MS15	1	1	6.442	16.609	–	Mild
MS16	1	1	6.054	16.609	–	Mild
MS17	0	3	6.513	16.609	–	Mild
MS18	1	1	7.177	16.609	–	Mild
MS19	1	0	6.26	16.609	–	Mild
MS20	2	0	4.909	27.87	–	Mild
MS21	0	1	3.77	28.891	–	Mild
MS22	1	0	6.429	16.609	–	Mild
MS23	1	0	5.52	16.609	–	Mild
MS24	1	0	4.739	31.664	–	Mild
MS25	1	1	5.357	16.609	–	Mild
MS26	1	0	6.007	16.609	–	Mild
MS27	1	0	5.278	37.424	–	Mild
MS28	1	0	5.278	37.424	–	Mild
MS29	1	0	5.504	25.539	–	Mild
MS30	1	0	4.963	19.961	–	Mild
MS31	2	0	5.215	19.961	–	Mild
MS32	2	0	4.626	43.149	–	Mild
MS33	1	0	4.003	23.314	–	Mild
MS34	2	0	5.415	59.432	–	Mild
MS35	1	1	4.781	43.149	–	Mild
MS36	1	0	6.185	16.609	–	Mild
MS37	2	0	5.581	51.21	–	Mild
MS38	2	0	4.37	27.87	–	Mild
MS39	1	1	4.162	16.609	–	Mild
MS40	1	0	6.192	23.314	–	Mild

J = 9 Hz, 2H, arom. H), 7.37 (d, J = 3 Hz, 2H, Ethylene), 7.45 (*t*, *J* = 3 Hz, 3H, arom. H), 7.67 (t, J = 6 Hz 2H, Benzimidazole), 7.25 (d, J = 9 Hz, 2H, Benzimidazole). **^{13}C NMR** (100 MHz, DMSO-*d6*) δ ppm: 137.10, 135.89, 128.96, 133.31, 123.92, 126.60, 142.73. **Mass:** 331.90 $(M+H)^+$.

((E)-1-(4-bromophenyl)-2-styryl-1H-benzo[d]imidazole) (MS-8)

Solubility: Ethanol, Acetic acid, Chloroform, 1,4-dioxane, DMSO; **R_f value:** 0.27; **M.P:** 210 °C; **UV λ_{max}** (Ethanol): 262.60/ 209.40; **FTIR** (cm^{-1}): 1494.01 (C = C stretch, aromatic), 1531.22 (C–C stretch, aromatic),

Table 4 RMSD calculation against 2Z5X

Sl No	Ligands	Reference	RMSD Value
1	HMN 1	HMN xray 6	0.6223
2	HMN 2	HMN xray 6	0.6221
3	HMN 3	HMN xray 6	0.6220
4	HMN 4	HMN xray 6	0.6221
5	HMN 5	HMN xray 6	0.6221
6	HMN xray 6	HMN xray 6	0.0000

Table 5 RMSD calculation against 1S3E

Sl No	Ligands	Reference	RMSD value
1	RHP601 1	RHP601 REF 6	0.6971
2	RHP601 2	RHP601 REF 6	1.5405
3	RHP601 3	RHP601 REF 6	1.5405
4	RHP601 4	RHP601 REF 6	1.5405
5	RHP601 5	RHP601 REF 6	1.5405
6	RHP601 REF 6	RHP601 REF 6	0.0000

Table 6 Molecular docking results of designed ligands against MAO-A and MAO-B

Sl No	Compound code	Binding Energy (-kcal/mol)	
		MAO-A (2Z5X)	MAO-B (1S3E)
1	MS1	53.32709	64.07646
2	MS2	56.13624	76.78583
3	MS3	114.89789	73.23463
4	MS4	53.86427	81.47093
5	MS5	79.13080	76.61092
6	MS6	71.0277	72.67619
7	MS7	76.74543	84.53666
8	MS8	60.03169	110.21145
9	Harmine/HRP	185.06253	169.62558

1282.24 (C-N stretch, aromatic), 3052.23 (C-H stretch, aromatic), 1621.52 (C=C stretch, aliphatic), 2968.07 (C-H stretch, aliphatic), 805.35 (C-H bend, aromatic), 695.53 (C–Br stretch, halogen). **^{1}H NMR** (300 MHz, DMSO): δ, ppm: 7.15 (d, J=3 Hz, 4H, bromobenzene), 7.31 (d, J=3 Hz, 2H, arom. H), 7.38 (d, J=3 Hz, 2H, Ethylene), 7.54 (t, J=3 Hz, 3H, arom. H), 7.69 (t, J=3 Hz 2H, Benzimidazole), 7.47 (d, J=3 Hz, 2H, Benzimidazole). **^{13}C NMR** (100 MHz, DMSO-*d6*) δ ppm: 142.73, 135.89, 126.63, 132.51, 137.74, 121.06, 112.46. **Mass:** 376.04 $(M+H)^{+}$.

In-vitro anti-depressant activity of the synthesized compounds

Determination of protein concentration

As described in the materials and methods section, the MAO protein concentration in the test sample was determined by plotting a standard curve (Fig. 5) between absorbance and concentration, which was found to be 189.51 µg/mL.

DNPH Spectrophotometry

The DNPH spectrophotometric analysis was first carried out without the presence of any drug that had resulted the absorbance reading of the control at 425 nm and at 465 nm (A_0). The steps of this method were repeated for the standard drug rasagiline as well as the test compounds MS 1 to MS 8 at various concentrations. Therefore, for each concentration of the standard drug rasagiline and the test compounds two values of absorbance (A_1) were recorded at 425 nm and at 465 nm (Additional file 1: Table 8). From the absorbances, % inhibition of MAO-A and MAO-B was calculated using the equation % inhibition = $[\{(A_0\text{-}A_1)/A_0\}\times 100]$, where, A_0 = Absorbance of control and A_1 = Absorbance of sample [22]. These % inhibition values (Additional file 1: Table 8) were plotted against the log concentration to obtain the dose response curve of rasagiline as well as the synthesized compounds against MAO-A (Additional file 1: Fig. 7) and against MAO-B (Additional file 1: Fig. 8). Then concentration of the test solutions that inhibit the hydrolysis of the substrate by 50% (IC_{50}) were determined by nonlinear regression using log dose vs. normalized response-variable slope by GraphPad Prism 9 (Additional file 1: Table 9).

To bridge the gap between computational findings and real-world applications, at the very beginning of docking, the root mean square deviation (RMSD) was calculated between the docked pose and X-ray pose of co-crystallized ligand. This is tabulated in Table 4 and 5. If the RMSD is less than 2 Å, it was considered that docking was successful and the compounds were docked in the exact place where the co-crystallized ligand was bound.

Structure activity relationship studies

From the in-vitro antidepressant assay and from the docking studies, it was observed that the compound MS-3 had the highest negative binding energy against 2Z5X and lowest IC_{50} value against MAO-A. Whereas the compound MS-8 had the highest negative binding energy against 1S3E and lowest IC_{50} value against MAO-B. The IC_{50} values for the other compounds

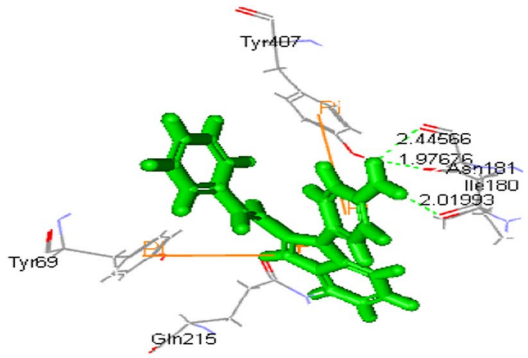

MS-1

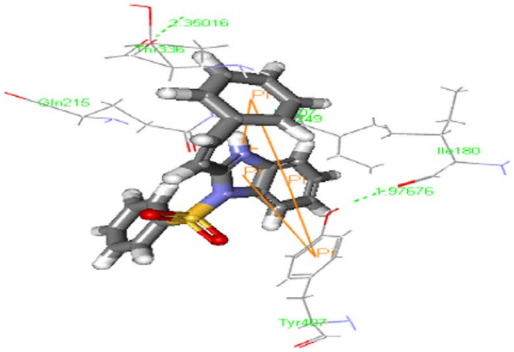

MS-2

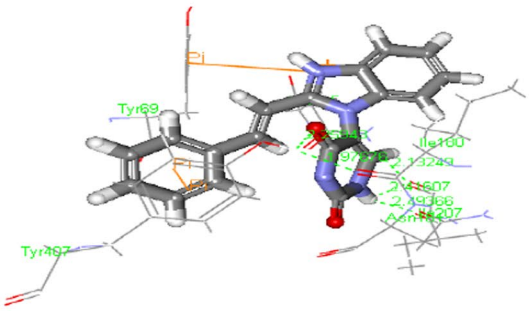

MS-3

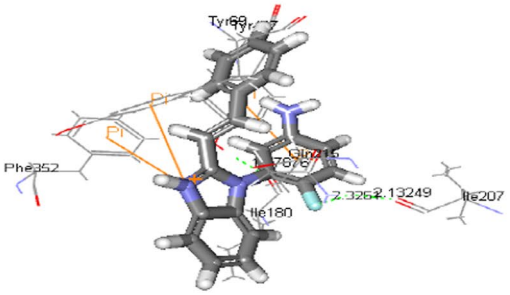

MS-4

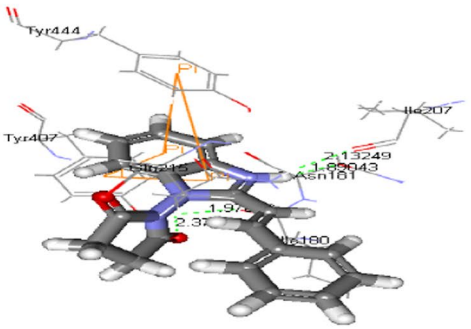

MS-5

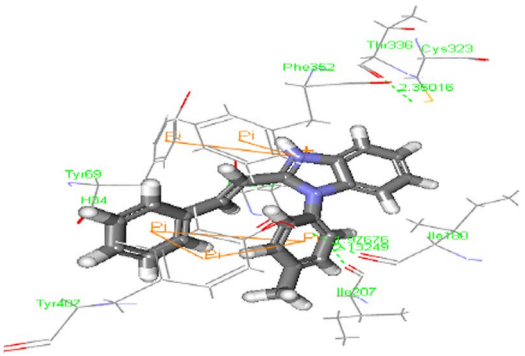

MS-6

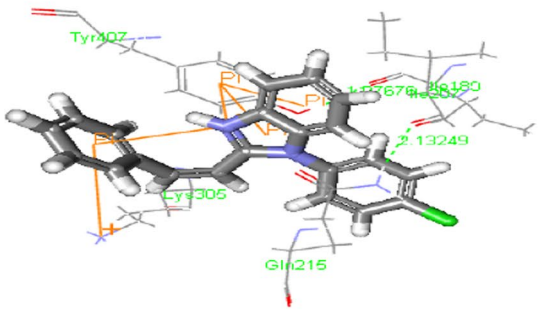

MS-7

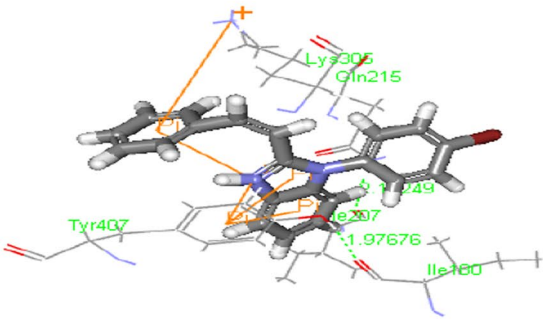

MS-8

Fig. 3 Interaction of ligands against protein 2Z5X

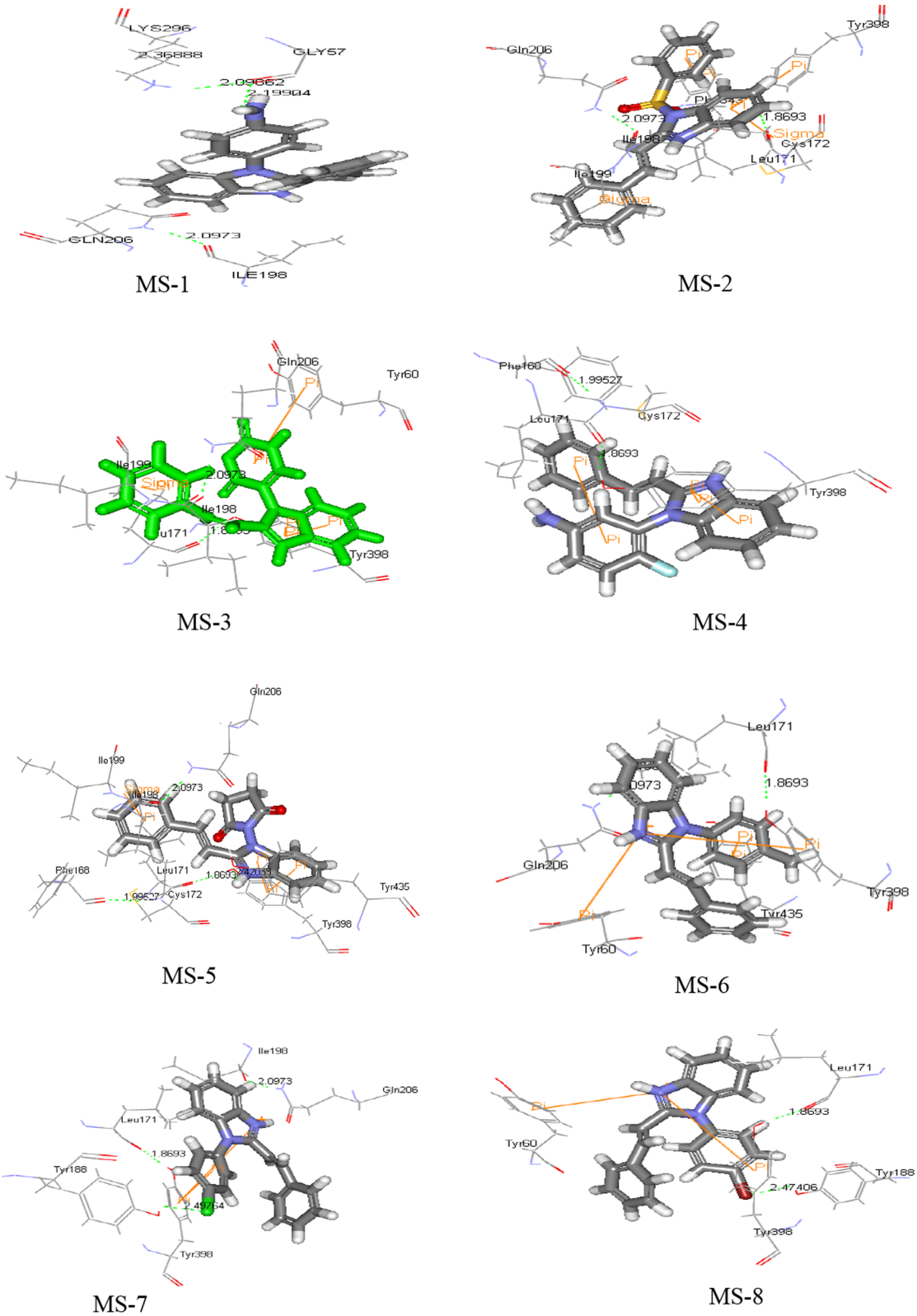

Fig. 4 Interaction of ligands against protein 1S3E

Table 7 Docking interactions of all the synthesized compounds for both the proteins viz.2Z5X (MAO-A) and 1S3E (MAO-B)

Compound codes	Docking interactions	
	MAO- A (2Z5X)	MAO- B (1S3E)
MS-1	Tyr407, Asn181, Ile180, Tyr69, Gln215	Lys296, Gly57, Gln206, Ile198
MS-2	Thr336, Gln216, Tyr407, Ile180	Gln206, Ile198, Ile199, Tyr398, Cys172, Leu171
MS-3	Tyr69, Tyr407, Ile180, Asn104	Ile199, Ile198, Gln206, Tyr398, Tyr60
MS-4	Phe352, Tyr69, Tyr407, Gln215, Ile180, Ile207	Phe168, Leu171, Cys172, Tyr398
MS-5	Tyr444, Tyr407, Gln215, Asn181, Ile207, Ile180	Ile199, Ile198, Phe168, Leu171, Cys172, Gln206, Tyr398, Tyr435
MS-6	Tyr69, Tyr407, Phe352, Ile207, Ile180, Thr336, Cys323	Leu171, Gln206, Tyr60, Tyr435, Tyr398
MS-7	Tyr407, Lys305, Gln215, Ile180	Leu171, Tyr188, Ile198, Tyr398, Gln206
MS-8	Tyr407, Lys305, Gln215, Ile207, Ile180	Tyr60, Leu171, Tyr188, Tyr398

Table 8 IC_{50} values obtained for all the synthesized compounds for both MAO-A and MAO-B

Compounds	IC_{50} (μM/mL)	
	For MAO-A	For MAO-B
MS-1	1051.44	605.04
MS-2	629.24	332.10
MS-3	367.19	430.76
MS-4	900.50	300.42
MS-5	492.53	387.28
MS-6	661.74	497.76
MS-7	536.25	239.04
MS-8	562.01	184.56
Rasagiline	559.163	93.32

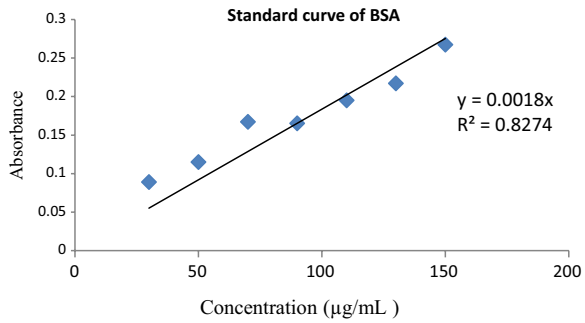

Fig. 5 BSA standard curve

were in accordance with the docking results. For all the compounds under investigation, it can be concluded that, lower is the IC_{50} value higher is the negative binding energy. The IC_{50} values of MS-3 and MS-8 against MAO-A and MAO-B, respectively, were comparable with that of the standard drug rasagiline.

From this study, it can be suggested that incorporation of nitrogen/oxygen substituted five- or six-member ring in the N^1 position of 2-styrylbenzimidazole derivatives which can exhibit different interactions with amino acid residues Ile180, Ile207 and Tyr407 might help in developing promising MAO-A inhibitors. Whereas incorporation of 4-halogen containing phenyl ring in the N^1 position of 2-styrylbenzimidazole derivatives which can exhibit different interactions with amino acid residues Leu171 and Tyr398 might help in developing promising MAO-B inhibitors.

Discussion

The docking study of MS-3 against the MAO-A protein 2Z5X suggested the presence of two pi–pi interaction with amino acids Tyr69 (linked with benzimidazole ring) and Tyr407 (linked with the benzene ring of cinnamic acid). It also suggested the presence of five hydrogen-bonded interaction with amino acids Ile180, Asn184and Ile207 of 2Z5X (Fig. 3). The oxygen and the nitrogen of the uracil ring which was present in the N^1 position of MS-3 were actively involved in formation of these hydrogen-bonded interaction. The next better IC_{50} value as well as binding energy against MAO-A and 2Z5X was observed for the compound MS-5, which also had oxygen and nitrogen atoms in a five membered succinimide ring present as a substitution in the N^1 position of MS-5. Two pairs of pi–pi interaction with the amino acids Tyr407, Tyr444 and four hydrogen-bonded interactions with the amino acids Gln215, Ile180, Asn181, Ile207 were observed in the binding pocket of MS-5 (Fig. 3). All the other synthesized compounds does not possess any nitrogen and oxygen containing ring substitutions which might be the reason of poor IC_{50} value of all other synthesized compounds against MAO-A. Some common amino acid residues like Tyr407, Ile 207 and Ile180 were involved in the binding pocket of most of the compounds

under investigation as well as the standard Harmine (Additional file 1: Fig. 5). The compounds MS3, MS5 and MS7 were showing better activity that of the standard drug rasagiline. The decreasing order of antidepressant activity of the synthesized compounds against MAO-A can be represented as:

$$MS3 > MS5 > MS7 > MS8 > MS2 > MS6 > MS4 > MS1$$

The docking study of MS-8 against the MAO-B protein 1S3E suggested the presence of two pi−pi interaction with amino acids Tyr60 and Tyr398 (both were linked with benzimidazole ring). It also suggested the presence of two hydrogen-bonded interaction with amino acids Leu171 and Tyr188 of 1S3E (Fig. 4). The bromine and the hydrogen of the bromobenzene ring which was present in the N^1 position of MS-8 were actively involved in formation of these hydrogen-bonded interaction. The next better IC_{50} value as well as binding energy against MAO-B and 1S3E was observed for the compound MS-7, which also had chlorine and hydrogen atoms in chlorobenzene ring present as a substitution in the N^1 position of MS-7. One pair of pi−pi interaction with amino acid Tyr398 and three hydrogen-bonded interactions with the amino acids Gln206, Leu171 and Tyr398 were observed in the binding pocket of MS-7 (Fig. 4). The compound MS-4 also possesses a fluorine atom in the ortho-position (with respect to the bond of joining of the aniline ring to benzimidazole ring) of the substituted aniline ring which might be the reason of its non-involvement in any kind of interaction with the protein 1S3E. Whereas the fluorine atom in MS-4 might be required for the additional stability of the compound in the binding pocket of 1S3E, depicted by the third better IC_{50} value against MAO-B. The IC_{50} values of all the other synthesized compounds were very high which might be due to the absence of any halogen atom in the 4th position of the substituted ring. The common amino acid residues involved in the binding pocket of other synthesized compounds and standard drug RHP (Fig. 4) with 1S3E were Leu171 and Tyr398. MS8 had shown comparable activity as that of the standard drug rasagiline. The decreasing order of antidepressant activity of the synthesized compounds against MAO-B can be represented as:

$$MS8 > MS7 > MS4 > MS2 > MS5 > MS3 > MS6 > MS1$$

Conclusion

The docking study of the synthesized compounds had shown interaction with similar amino acid residues with that of the X-ray pose co-crystallized ligands like RHP and Harmine. This finding might pave the way for the development of 2-styrylbenzimidazole derivatives as potent antidepressants. The compounds MS-3 and MS-8 had shown good antidepressant activity by inhibiting MAO-A and MAO-B, respectively. The optimization of the designed 2-styrylbenzimidazole derivatives with the structural findings of the present work might lead to the development of novel and potent antidepressant drugs.

Abbreviations

ADMET	Absorption, distribution, metabolism, excretion, and toxicity
FTIR	Fourier transform infrared
^{1}H-NMR	Proton nuclear magnetic resonance
^{13}C-NMR	Carbon-13 nuclear magnetic resonance
DNPH	2,4-Dinitrophenylhydrazine
MAO-A	Monoamine oxidase A
MAO-B	Monoamine oxidase B
GHDx	Global health data exchange
SSRIs	Selective serotonin reuptake inhibitors
5-HT receptor antagonists	5-Hydroxytryptamine receptor antagonists
MAOIs	Monoamine oxidase inhibitors
TCAs	Tricyclic antidepressants
TPSA	Total polar surface area
nRB	Number of rotatable bond
HBD	Hydrogen bond donor
HBA	Hydrogen bond acceptor
PSA-2D	2D polar surface area
TOPKAT	Toxicity prediction by komputer assisted technology
PDB	Protein data bank
RHP	5-Hydroxy-N-propargyl-1(R)-aminoindan
RMSD	Root mean square deviation
DMSO	Dimethyl sulfoxide
BSA	Bovine serum albumin
NMR	Nuclear magnetic resonance
THF	Tetrahydrofuran
NaOH	Sodium hydroxide
R_f	Retardation factor
M.P	Melting point

Supplementary Information

The online version contains supplementary material available at https://doi.org/10.1186/s43094-024-00589-2.

Additional file 1: Fig. 7. Dose-Response curve between the % inhibition of MAO-A vs. log concentration (µg/mL) of Rasagiline and the test compounds (MS-1 to MS-8). **Fig. 8**. Dose-Response curve between the % inhibition of MAO-B vs. log concentration (µg/mL) of Rasagiline and the test compounds (MS-1 to MS-8)

Acknowledgements

Authors are thankful to Dr. Anshul Shakya, Assistant Professor, Department of Pharmaceutical Sciences, Dibrugarh University for his constant guidance to carry out the in-vitro antidepressant assay. The infrastructural facility and the sophisticated instrumental facility provided by Dibrugarh University, Dibrugarh, Assam to carry out the work is gratefully acknowledged.

Author contributions

MS carried out the synthetic and *in-vitro* work. RC was involved in the *in-silico study*. PP interpreted the FTIR spectral data and the in-vitro results. FA interpreted the NMR spectral data. RSD was involved in manuscript writing and language editing. SS was involved in the study concept, study design and editing of the manuscript.

Funding

Not applicable.

Availability of data and materials
The data that support the findings of this study are available from the corresponding author, upon reasonable request.

Declarations

Ethics approval and consent to participate
Not applicable.

Competing interests
The authors declare that they have no competing interests.

Author details
[1]Department of Pharmaceutical Sciences, Faculty of Science and Engineering, Dibrugarh University, Dibrugarh, Assam 786004, India. [2]School of Pharmaceutical Sciences, Girijananda Chowdhury Institute of Pharmaceutical Sciences-Tezpur, Girijananda Chowdhury University, Tezpur Campus, Guwahati, Assam 784501, India.

Received: 22 June 2023 Accepted: 29 January 2024
Published online: 15 February 2024

References

1. GBD (2019) Healthcare Access and Quality Collaborators (2022) Assessing performance of the Healthcare Access and Quality Index, overall and by select age groups, for 204 countries and territories, 1990–2019: a systematic analysis from the Global Burden of Disease Study 2019. Lancet Glob Health 10:E1715–E1743. https://doi.org/10.1016/S2214-109X(22)00429-6
2. WHO fact sheets (2023) https://www.who.int/news-room/fact-sheets/detail/depression. Accessed 15 June 2023
3. Tonelli M, Paglietti G, Boido V, Sparatore F, Marongiu F, Marongiu E, La Colla P, Loddo R (2008) Antiviral activity of benzimidazole derivatives. I. Antiviral Activity of 1-Substituted-2-[(Benzotriazol-1/2-yl)methyl] benzimidazoles. Chem Biodivers 5:2386–2401. https://doi.org/10.1002/cbdv.200890203
4. Tonelli M, Simone M, Tasso B et al (2010) Antiviral activity of benzimidazole derivatives. II. Antiviral activity of 2-phenylbenzimidazole derivatives. Bioorganic Med Chem 18:2937–2953. https://doi.org/10.1016/j.bmc.2010.02.037
5. Vitale G, Corona P, Loriga M, Carta A, Paglietti G, Giliberti G, Sanna G, Farci P, Marongiu ME, La Colla P (2012) 5-Acetyl-2-arylbenzimidazoles as antiviral agents. Part 4. Eur J Med Chem 53:83–97. https://doi.org/10.1016/j.ejmech.2012.03.038
6. Francesconi V, Cichero E, Schenone S, Naesens L, Tonelli M (2020) Synthesis and biological evaluation of novel (thio)semicarbazone-based benzimidazoles as antiviral agents against human respiratory viruses. Molecules 25:1487. https://doi.org/10.3390/molecules25071487
7. Özkay Y, Tunall Y, Karaca H, Işlkdağ I (2011) Antimicrobial activity of a new series of benzimidazole derivatives. Arch Pharm Res 34:1427–1435. https://doi.org/10.1007/s12272-011-0903-8
8. Özkay Y, Tunalı Y, Karaca H, Işıkdağ İ (2011) Antimicrobial activity of a new combination system of benzimidazole and various azoles. Arch Pharm (Weinheim) 344:264–271. https://doi.org/10.1002/ardp.201000172
9. Hosamani KM, Shingalapur RV (2011) Synthesis of 2-mercaptobenzimidazole derivatives as potential anti-microbial and cytotoxic agents. Arch Pharm (Weinheim) 344:311–319. https://doi.org/10.1002/ardp.200900291
10. Song D, Ma S (2016) Recent development of benzimidazole-containing antibacterial agents. Chem Med Chem 11:646–659. https://doi.org/10.1002/cmdc.201600041
11. Brishty SR, Hossain MJ, Khandaker MU, Faruque MRI, Osman H, Rahman SMA (2021) A comprehensive account on recent progress in pharmacological activities of benzimidazole derivatives. Front Pharmacol 12:762807. https://doi.org/10.3389/fphar.2021.762807
12. El Rashedy AA, Aboul-Enein HY (2013) Benzimidazole derivatives as potential anticancer agents. Mini Rev Med Chem 13:399–407. https://doi.org/10.2174/138955713804999847
13. Yadav S, NarasimhanKaur BH (2016) Perspectives of benzimidazole derivatives as anticancer agents in the New Era. Anticancer Agents Med Chem 16:1403–1425. https://doi.org/10.2174/1871520616666151103113412
14. Kumar A, Banerjee S, Roy P, Sondhi SM, Sharma A (2018) Solvent-free synthesis and anticancer activity evaluation of benzimidazole and perimidine derivatives. Mol Divers 22:113–127. https://doi.org/10.1007/s11030-017-9790-3
15. El-Nassan HB (2012) Synthesis, antitumor activity and SAR study of novel [1,2,4]triazino[4,5-a] benzimidazole derivatives. Eur J Med Chem 53:22–27. https://doi.org/10.1016/j.ejmech.2012.03.028
16. Kumar R, Singh C, Mazumder A, Salahuddin AMM, Kumar V, Giri PP (2021) Synthetic approach to potential anticancer benzimidazole derivatives: a review. Mini Rev Med Chem 22:1289–1304. https://doi.org/10.2174/1389557521666211001122118
17. Dik B, Coşkun D, Bahçivan E, Üney K (2021) Potential antidiabetic activity of benzimidazole derivative albendazole and lansoprazole drugs in different doses in experimental type 2 diabetic rats. Turkish J Med Sci 51:1579–1586. https://doi.org/10.3906/sag-2004-38
18. El Bakri Y, Anouar EH, Marmouzi I, Sayah K, Ramli Y, El Abbes FM, Essassi EM, Mague JT (2018) Potential antidiabetic activity and molecular docking studies of novel synthesized 3.6-dimethyl-5-oxo-pyrido[3,4-f][1,2,4]triazepino[2,3-a]benzimidazole and 10-amino-2-methyl-4-oxo pyrimido[1,2-a]benzimidazole derivatives. J Mol Model 24:1–10. https://doi.org/10.1007/s00894-018-3705-9
19. Spasov AA, Vassiliev MP, Anisimova AV, Zhukovskaya NO (2019) Antidiabetogenic features of benzimidazoles. In: Marinescu M (ed) Chemistry and applications of benzimidazole and its derivatives. Intech Open. doi:https://doi.org/10.5772/intechopen.84802
20. Tantray MA, Khan I, Hamid H, Alam MS, Dhulap A, Kalam A (2018) Synthesis of benzimidazole-linked-1,3,4-oxadiazole carboxamides as GSK-3β inhibitors with in vivo antidepressant activity. Bioorg Chem 77:393–401. https://doi.org/10.1016/j.bioorg.2018.01.040
21. Tantray MA, Khan I, Hamid H, Alam MS, Dhulap A, Kalam A (2016) Synthesis of benzimidazole-based 1,3,4-oxadiazole-1,2,3-triazole conjugates as glycogen synthase kinase-3β inhibitors with antidepressant activity. In vivo models RSC Adv 6:43345–43355. https://doi.org/10.1016/j.bioorg.2018.01.040
22. Tian Y, Liu W, Lu Y et al (2016) Naturally occurring cinnamic acid sugar ester derivatives. Molecules 21:1402. https://doi.org/10.3390/molecules21101402
23. Da Silveira E, Sá RDC, Andrade LN, De Oliveira RDRB, De Sousa DP (2014) A review on anti-inflammatory activity of phenylpropanoids found in essential oils. Molecules 19:1459–1480. https://doi.org/10.3390/molecules19021459
24. Sova M (2012) Antioxidant and antimicrobial activities of cinnamic acid derivatives. Mini-Reviews Med Chem 12:749–767. https://doi.org/10.2174/138955712801264792
25. Anantharaju PG, Gowda PC, Vimalambike MG, Madhunapantula SV (2016) An overview on the role of dietary phenolics for the treatment of cancers. Nutr J 15:1–16. https://doi.org/10.1186/s12937-016-0217-2
26. Alam MA, Subhan N, Hossain H, Hossain M, Reza HM, Rahman MM, Ullah MO (2016) Hydroxycinnamic acid derivatives: a potential class of natural compounds for the management of lipid metabolism and obesity. Nutr Metab 13:1–13. https://doi.org/10.1186/s12986-016-0080-3
27. Liu P, Hu Y, Guo DH, Wang DX, Tu HH, Ma L, Xie TT, Kong LY (2010) Potential antidepressant properties of Radix Polygalae (Yuan Zhi). Phytomedicine 17:794–799. https://doi.org/10.1016/j.phymed.2010.01.004
28. Szwajgier D, Borowiec K, Pustelniak K (2017) The neuroprotective effects of phenolic acids: Molecular mechanism of action. Nutrients 9:1–21. https://doi.org/10.3390/nu9050477
29. Diniz LRL, de Souza MT S, Barboza JN, de Almeida RN, de Sousa DP (2019) Antidepressant potential of cinnamic acids: drug development. Molecules 24(1):12. https://doi.org/10.3390/molecules24244469
30. Shingalapur RV, Hosamani KM, Keri RS (2009) Synthesis and evaluation of in vitro anti-microbial and anti-tubercular activity of 2-styryl

benzimidazoles. Eur J Med Chem 44:4244–4248. https://doi.org/10.1016/j.ejmech.2009.05.021
31. Egan WJ, Lauri G (2002) Prediction of intestinal permeability. Adv Drug Deliv Rev 54:273–289. https://doi.org/10.1016/s0169-409x(02)00004-2
32. Cheng A, Merz KM (2003) Prediction of aqueous solubility of a diverse set of compounds using quantitative structure-property relationships. J Med Chem 46:3572–3580. https://doi.org/10.1021/jm020266b
33. Son S-Y, Ma J, Kondou Y, Yoshimura M, Yamashita E, Tsukihara T (2008) Human monoamine oxidase A: structure and control of opening the entry for substrates/inhibitors. Acta Crystallogr Sect A Found Crystallogr 64:C457–C457. https://doi.org/10.1107/S0108767308085322
34. Binda C, Hubálek F, Li M, Herzig Y, Sterling J, Edmondson DE, Mattevi A (2004) Crystal structures of Monoamine Oxidase B in complex with four inhibitors of the N-propargylaminoindan class. J Med Chem 47:1767–1774. https://doi.org/10.1021/jm031087c
35. Wu G, Robertson DH, Brooks CL, Vieth M (2003) Detailed analysis of grid-based molecular docking: a case study of CDOCKER—A CHARMm-based MD docking algorithm. J Comput Chem 24:1549–1562. https://doi.org/10.1002/jcc.10306

Publisher's Note